University of Wisconsin Madison

Collider Physics 835 Presentation

Electroweak Triple Gauge Coupling and New Physics

Author:
Rich Ormiston

May 18, 2013

1 The Process

The object of this search is to not only demonstrate the electroweak triple gauge couple of vector bosons that naturally results from the construction of a non-Abelian gauge theory, but to then use methods from effective field theory to investigate this vertex further. There are five dimension-6 operators which can be used to fit multiple parameters of the WWZ lagrangian to regular SM predictions. The fully leptonic decays of the W-bosons have a rather low branching ratio, $\Gamma(W \to l\nu) \approx 11\%$, the signal to background ratio is quite good and the background signals that remain are not so terrible to contend with.

The coupling parameters being applied here are established in the 2012 PDG maintain only 68% CL, and we will see the effects of such parameters. The terms which stray from those of the SM have couplings which are very near (or possibly) zero, but it will not be until future colliders are able to establish a higher level of accuracy, we will not know if 'near zero' is actually zero. In what follows, a tree level analysis will be considered. We can still demonstrate a conservation of unitary at this level so long as the virtual Z indeed exists. Therefore establishing the WW production is important for solidifying and reaffirming the electroweak GSM theory.

1.1 Demonstration of Conservation of Unitary

The amplitudes for the two s-channel (ignoring the Higgs contribution since $\mathcal{M}_{\mathcal{H}} \propto m_e \to 0$) and one t-channel diagrams for the production of an on-shell WW boson pair are

$$\mathcal{M}_\nu = -i\frac{(-ig_W^2)}{8M_W^2}\bar{\nu}(p_+)(\not{k}_+ - \not{k}_-)(1-\gamma_5)u(p_-) \tag{1}$$

$$\mathcal{M}_\gamma = -i\frac{g_W^2 Q_e \sin^2\theta_W}{(k_- + k_+)^2}\,\bar{\nu}\gamma_\rho u(p_-)\, g^{\rho\mu}\,\Gamma_{\mu\alpha\beta}(q,k_-,k_+)\epsilon^\alpha(k_-)\epsilon^\beta(k_+) \tag{2}$$

$$\mathcal{M}_{\mathcal{Z}} = -i\frac{g_W^2}{2[(k_- + k_+)^2 - M_Z^2]}\,\bar{\nu}\gamma_\rho(c_V^e - c_A^e\gamma_5)u(p_-)\, g^{\rho\mu}\,\Gamma_{\mu\alpha\beta}(q,k_-,k_+)\epsilon^\alpha(k_-)\epsilon^\beta(k_+) \tag{3}$$

with

$$\Gamma_{\mu\alpha\beta}(q,k_-,k_+)\epsilon^\alpha(k_-)\epsilon^\beta(k_+) = -\frac{(k_- + k_+)^2}{2M_W^2}(k_+ - k_-)_\mu \tag{4}$$

where the polarization vectors were taken to be

$$\epsilon_L^\mu(k_\pm) = (\frac{k}{M_W}, 0, 0, \pm\frac{E}{M_W}) \rightarrow \epsilon_L^\mu \approx \frac{1}{M_W}\left(k_\pm - \frac{M_W^2}{2E^2}k_\mp\right) \tag{5}$$

Therefore one may show that

$$\mathcal{M}_\gamma + \mathcal{M}_\mathcal{Z} = i\frac{(-ig_W^2)}{8M_W^2}\bar{\nu}(p_+)(\not{k}_+ - \not{k}_-)(1-\gamma_5)u(p_-) \tag{6}$$

and so finally

$$\mathcal{M}_\gamma + \mathcal{M}_\mathcal{Z} + \mathcal{M}_\nu = 0 \tag{7}$$

So the 'bad s' behavior is subdued by the inclusion of the massive vector boson. It is not until we get to $4\pi v \approx 3TeV$ for Λ where v is the vacuum expectation value, that we need to consider the Higgs contribution in order to preserve the correct behavior of the cross section. At the CM energies here, it may be safely neglected.

2 The Process

The search here is for the production of a W-boson pair via an $e + e-$ in-state. The W's will decay either leptonically or hadronically resulting in fully hadronic, fully leptonic, or mixed leptonic and hadronic final states. There are definite pros and cons to each channel. The fully leptonic channel is $\sim 95\%$ pure though $\Gamma(W \rightarrow l\nu) \approx 11\%$ so the branching ratio is unfortunately low. Additionally the MET is rather high due to the 2 neutrinos in the final state and worse, if one of the leptons is a τ, we will have another lepton in the final state creating a MET that is impossible to reconstruct. The fully hadronic decay will have 3 jet pairing options since we do not know what the initial flavors are. It is the dominant process, although it is also the least sensitive to the deviations of the anomalous coupling that will be implemented here. The diagrams are as follows:

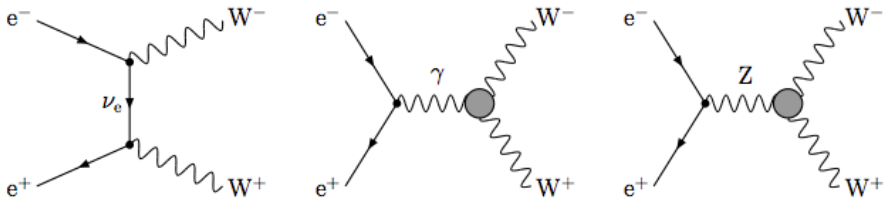

3 The Lagrangian

Most general Lagrangian for the TGC interaction is

$$\mathcal{L} = ig_{WWZ}\Big[g_V^1(W^*_{\mu\nu}W^\mu V^\nu - W^{*\mu}W_{\mu\nu}V^\nu) + k_V W^*_\mu W_\nu V^{\mu\nu} + \frac{\lambda_V}{M_W^2}W^*_{\alpha\mu}W^{\mu\nu}V^\alpha_\nu \tag{8}$$

$$+ig_V^4 W^*_\mu W_\nu(\partial^\mu V^\nu + \partial^\nu V^\mu) - ig_V^5\epsilon^{\mu\nu\rho\sigma}(W^*_\mu\partial_\rho W_\nu - \partial_\rho W^*_\mu W_\nu)V_\sigma \tag{9}$$

$$+\tilde{k}_V W^*_\mu W_\nu \tilde{V}^{\mu\nu} + \frac{\tilde{\lambda}_V}{M_W^2}W^*_{\alpha\mu}W^{\mu\nu}\tilde{V}^\alpha_\nu\Big] \tag{10}$$

There are fourteen parameters available ($V = \gamma$ and Z), which are far too many to handle at once so we must cut down on them and then adjust just one at a time and look at the resulting distributions to see what effects are caused and therefore where to begin looking for potential new physics. First, we may assume that the CP-violating parameters are zero here, so we're down to ten. Next, g_γ^4, g_γ^5 and λ_γ violate charge conjugation, thus in order to preserve electromagnetic gauge invariance, we demand these to be zero. Lastly, since g_V^1 alters the distributions very little, we need not consider it here. Therefore, we are left with five parameters.

In the SM, at tree level we use

$$\tilde{\lambda}_V = \lambda_V = \tilde{k}_V = g_V^4 = g_V^5 = 0, \quad k_V = 1 \tag{11}$$

and so all SM plots will use these values.

The 2012 PDG values for the anomalous gauge coupling parameters are given within a 68% confidence limit. They are shown in Fig. 2 and Fig. 1.

The coupling parameters shown are a great way to determine the electric quadrupole moment:

$$q_W = -\frac{e}{M_W^2}(\kappa_\gamma - \lambda_\gamma) \xrightarrow{SM} -\frac{e}{M_W^2}(1-0) \tag{12}$$

and the magnetic dipole moment

$$\mu_W = \frac{e}{2M_W}(1+\kappa_\gamma+\lambda_\gamma) \xrightarrow{SM} \frac{e}{2M_W}(1+1+0) \tag{13}$$

The values shown in the table will be implemented primarily at their maximum and minimum values to show the maximum possible variation. Notice the definitions given are what is actually being implemented, though one may solve the equations for a given coupling. The scale factor Λ has the dimensions of mass and is usually placed around the $1-10$ TeV scale.

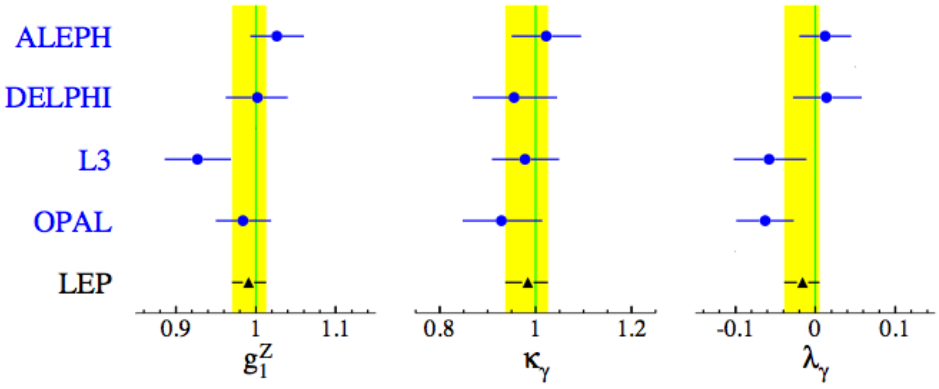

Figure 1: 68% CL of anomalous gauge coupling values

Couplings	Definition	2012 PDG Values
g_Z^1	$1 + c_W \frac{M_Z^2}{2\Lambda^2}$	$0.984^{+0.022}_{-0.019}$
κ_γ	$1 + (c_W + c_B)\frac{M_W^2}{2\Lambda^2}$	$0.973^{+0.044}_{-0.045}$
κ_Z	$1 + (c_W - c_B \tan^2\theta_W)\frac{M_W^2}{2\Lambda^2}$	$0.924^{+0.059}_{-0.056} \pm 0.024$
λ_Z	$c_{WWW}\frac{3g^2 M_W^2}{2\Lambda^2}$	$-0.088^{+0.060}_{-0.057} \pm 0.023$
$\tilde{\kappa}_Z$	$-c_{\tilde{Z}} \tan^2\theta_W \frac{M_W^2}{2\Lambda^2}$	$-0.12^{+0.06}_{-0.04}$
$\tilde{\lambda}_Z$	$c_{\tilde{W}WW}\frac{3g^2 M_W^2}{2\Lambda^2}$	-0.09 ± 0.07

Figure 2: Table showing the 2012 PDG values for the parameters and their definitions used here (sometimes the form $\mathcal{O}_{WWW}$ is used instead of c_{WWW})

3.1 Proving the Proper Cross Section Behavior

We can prove the good behavior of the cross section by assuming only

$$\lambda_V \neq 0, \quad k_V \neq 0 \tag{14}$$

Then the one loop, unpolarized cross section can be worked out to give

$$\frac{d\sigma}{d\Omega} = \frac{\alpha^2\beta}{32s_W^4 s}\left[\mathcal{M}_{\mathcal{Z}\mathcal{Z}} + \mathcal{M}_{\gamma\gamma} + \mathcal{M}_{\nu\nu} + \mathcal{M}_{\mathcal{Z}\nu} + \mathcal{M}_{\mathcal{Z}\gamma} + \mathcal{M}_{\gamma\nu}\right] \tag{15}$$

And

$$\mathcal{M}_{\gamma\gamma} = 4s_W^4 N_1(k_\gamma, k_\gamma; \lambda_\gamma, \lambda_\gamma) \tag{16}$$

$$\mathcal{M}_{\mathcal{Z}\mathcal{Z}} = \frac{s^2[1 + 4s_W^2(2s_W^2 - 1)]}{2[(s - M_Z^2)^2 + \Gamma_Z^2 M_Z^2]} N_1(k_Z, k_Z; \lambda_Z, \lambda_Z) \tag{17}$$

$$\mathcal{M}_{\gamma\mathcal{Z}} = \frac{2s^2(s - M_Z^2)[s_W^2(1 - 4s_W^2)]}{[(s - M_Z^2)^2 + \Gamma_Z^2 M_Z^2]} N_1(k_\gamma, k_Z; \lambda_\gamma, \lambda_Z) \tag{18}$$

$$\mathcal{M}_{\mathcal{Z}\nu} = \frac{s(s - M_Z^2)(2s_W^2 - 1)}{2[(s - M_Z^2)^2 + \Gamma_Z^2 M_Z^2]} N_2(k_Z, \lambda_Z) \tag{19}$$

$$\mathcal{M}_{\gamma\nu} = -s_W^2 N_2(k_\gamma, \lambda_\gamma) \tag{20}$$

$$\mathcal{M}_{\nu\nu} = N_3 \tag{21}$$

where

$$N_1(a, b; c, d) = F\left[(ab + 2cd)y^2 - [1 - d - c + (a + c)(b + d)]y + 3\right] \tag{22}$$

$$+2(1 + a + c)(1 + b + d)\beta^2 y \tag{23}$$

$$N_2(a, b) = 4Fy\left(ay - 1 - \frac{2M_W^2}{t}\right) + 8(1 + a + b)\left(1 + \beta^2 y + \frac{M_W^2}{t}\right) \tag{24}$$

$$N_3 = 4y + \frac{F}{2}\left(y^2 + \frac{4y^2 M_W^2}{t^2}\right) \tag{25}$$

And finally with

$$s = (p_+ + p_-)^2 \quad t = (k_+ - p_+)^2 \quad u = (k_+ - p_-)^2 \quad \beta^2 = 1 - 4y_V \tag{26}$$

$$F = \frac{1}{y^2}\left(\frac{ut}{M_W^4} - 1\right), \quad y_V = s/2M_V^2 = 1/2x_V, \;\; x_V = 4M_V^2/s \tag{27}$$

To avoid a horrendous amount more of analytical work, I've set the Dim. 6 coefficients to the SM tree-level values and Γ_Z to zero. Then turning $N_{1,2,3} \to D_{1,2,3}$ with

$$D_1(a,b;c,d) = \frac{4y\beta^2}{3}\left\{y(ab+2cd) + 2[1+2d+2c+(a+c)(b+d)+\frac{3}{2}(a+b)] + 4\right\} \tag{28}$$

$$D_2(a,b) = 8\beta^2 y\left(2a+2b+\frac{5}{3}+\frac{ay}{3}\right) + 16(1+a+b)\left(1-\frac{1}{\beta y}\ln\frac{1+\beta}{1-\beta}\right) \tag{29}$$

$$-\frac{8}{\beta y^2}\ln\frac{1+\beta}{1-\beta} + 4(1+\beta^2) \tag{30}$$

$$D_3 = 8 + \frac{4(1+\beta^2)}{\beta}\ln\frac{1+\beta}{1-\beta} + 2\beta^2 y\left(4+\frac{y}{3}\right) \tag{31}$$

After a fair amount of algebra we end up with

$$\sigma^{CM} = \frac{\pi\alpha^2\beta}{2s_W^4 s}\left\{\frac{1}{\beta}\left(1+\frac{2}{y}+\frac{2}{y^2}\right)\ln\frac{1+\beta}{1-\beta}\right.$$

$$\left.+\frac{M_Z^2(1-2s_W^2)}{s-M_Z^2}\left[\frac{2}{\beta y^2}(1+2y)\ln\frac{1+\beta}{1-\beta} - \frac{y}{12} - \frac{5}{3} - \frac{1}{y}\right] + \frac{M_Z^4(8s_W^4-4s_W^2+1)}{48(s-M_Z^2)^2}(y+20y+12)\right\}$$

The maximum cross section is at $\approx$ 200 GeV and decreases like $\sigma^{CM} \approx \frac{\ln s}{s}$, thus explicitly showing the behavior at large $\hat{s}$ even at the loop level. This analysis will be concerned with CM energies then, at 200 GeV.

4 Vertex Corrections

The initial vertex becomes altered by use of the new Lagrangian to derive the Feynman rules in the following way:

$$\Gamma^{\alpha\beta\mu}(q,k,p) = g^{\alpha\mu}(q+k)^{\beta} + g^{\beta\mu}(p-k)^{\alpha} - g^{\alpha\beta}(p+q)^{\mu} \rightarrow \tag{32}$$

$$\Gamma_V^{\alpha\beta\mu}(q,k,p) = f_V^1(q-k)^{\mu}g^{\alpha\beta} - \frac{f_V^2}{M_W^2}(q-k)^{\mu}p^{\alpha}p^{\beta} + f_V^3(p^{\alpha}g^{\mu\beta} - p^{\beta}g^{\mu\alpha})$$

$$+if_V^4(p^{\alpha}g^{\mu\beta} + p^{\beta}g^{\mu\alpha}) + if_V^5\epsilon^{\mu\alpha\beta\rho}(q-k)_{\rho} - f_V^6\epsilon^{\mu\alpha\beta\rho}p_{\rho}$$

$$-\frac{f_V^7}{M_W^2}(q-k)^{\mu}\epsilon^{\alpha\beta\rho\sigma}p_{\rho}(q-k)_{\sigma}$$

with

$$f_V^1 = g_V^1 + \frac{\hat{s}}{2M_W^2}\lambda_V, \quad f_V^2 = \lambda_V, \quad f_V^3 = g_V^1 + \kappa_V + \lambda_V, \quad f_V^4 = g_V^4,$$

$$f_V^5 = g_V^5, \quad f_V^6 = \tilde{\kappa}_V - \tilde{\lambda}_V, \quad f_V^7 = -\frac{1}{2}\tilde{\lambda}_V$$

The new vertex is written so that is maintains the same layout as the Lagrangian, which is the reason for the introduction of the f_V terms. It is important to note here $f_V^1 = g_V^1 + \frac{\hat{s}}{2M_W^2}\lambda_V$. This means that we will be able to observe stronger effects of the anomalous coupling parameters (namely, λ_V) as we move to higher energies. This behavior will be explicitly shown on a following distribution. Additionally, we employ the momenta of the bosons in a few arrangements, suggesting that the p_T distributions will be a good place to look for TGC sensitivity and potential new physics.

5 Signal and Background

5.1 ZZ production

If we operate at $\sqrt{s} \geq 182$ GeV (twice the Z mass), then it is possible to produce a pair of Z bosons. The cross section ranges from around 1.34 pb to 0.97 pb as we change from 209 to 189 GeV. The background is somewhat difficult to contend with since the Z's will decay leptonically and the final states contains four fermions. This will look similar to the

WW signature that we would expect. We will see clear evidence of the diboson production shortly. The leading diagrams are:

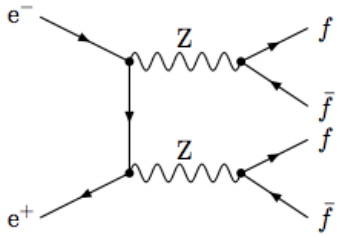

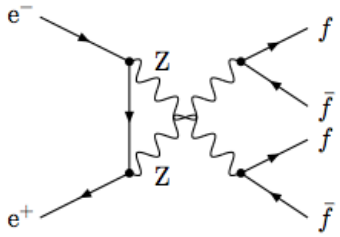

5.2 $ee \to f\bar{f}\gamma$

s-channel Bhabba scattering can occur where, when the CM energy is larger than the Z mass, hard photons can be radiated from the incoming electrons which effectively reduces the CM energy in a direction which increases the cross section, usually towards Z resonance, and is known as "radiative return to the Z." In a similar matter from QCD, if gluons are emitted, they form the primary $qqqq$ background.

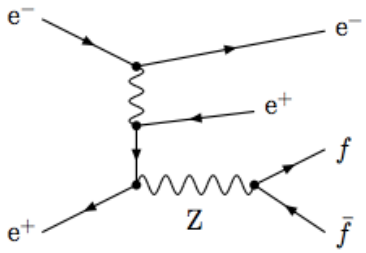

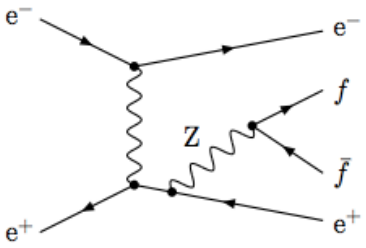

5.3 Single Z

The final state will contain the initial state particles ($e+$ and $e-$) and additionally two other fermions produced by the Z decay. These four fermion processes form an irreducible background, and what is typically done is a reweighing. One would calculate the square of the amplitude for the 4-fermion process and divide it by the square of the amplitude for the WW on-shell production, giving the new weight.

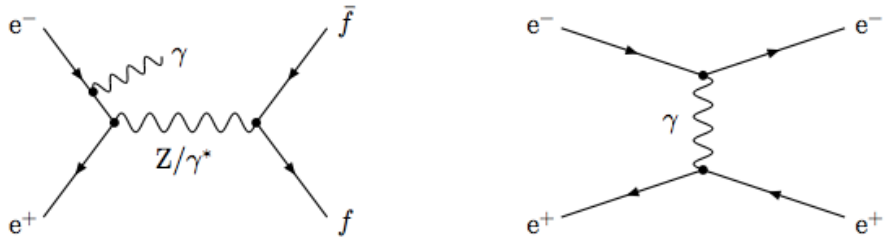

5.4 $t\bar{t} \to WWbb$

Final state leptons may be observed, but the b-quarks will result in jets deposited in the hadronic calorimeter. The signal will be easy to spot and fortunately, as we can use primarily $WW \to 2l2\nu$ and $WW \to q\bar{q}l\nu$, we have minimal work to do with the jets.

6 Simulation Cuts at $\sqrt{s} = 200$ GeV

The cuts for the p_T of the leading and trailing leptons are rather standard in $q\bar{q}e\nu$ channels. (leading $p_T \geq 20$ GeV, trailing $p_T \geq$ 10 GeV). Any events below the 10 GeV cut are not sensitive to the TGC vertex and so may be rejected. Additionally, $\simeq 60\%$ of WZ events are removed and $\simeq 10\%$ of ZZ events. To insure that the electron is indeed an isolated electron and not the result of a hadronic decay within a jet, we can require that the majority of the electron energy ($\sim$80 - 85%) is deposited within a cone of 15 degrees. In general, if a lepton is created within a jet, it will follow in the direction of the jet. However the angle can become large enough that the lepton is mistaken for an isolated event and counted. (Angle is from transverse plane)

In a decay to 2l2ν, we will expect quite a large MET due to the neutrinos. A comparison of the MET generated from qqqq, qqlν and 2l2ν will be shown. We will see that the MET from the 4 jet event is reduced by roughly 75% with a cut for MET$\geq$ 10GeV and reduced by about 95% when we cut MET$\geq$ 20 GeV. Similarly, the contribution from qqlν is reduced by $\sim$ 5% at MET$\geq$ 10 GeV and around 20% at MET$\geq$ 20 GeV. The fully leptonic channel only is reduced by $\sim$ 15% at a cut of 20 GeV. Thus, MET$\geq$ 20 GeV.

We can apply an invariant mass cut for a dimuon pair at $M_{\mu\mu} \leq 75$ GeV which enables a reduction in ZZ events (about 15 GeV below Z mass). And invariant mass less than or equal to 65 GeV for an eν pair is consistent then with W (on-shell) production.

7 A Quick Look at Backgrounds

One way to understand what we are eliminating from our desired process is to see it directly.

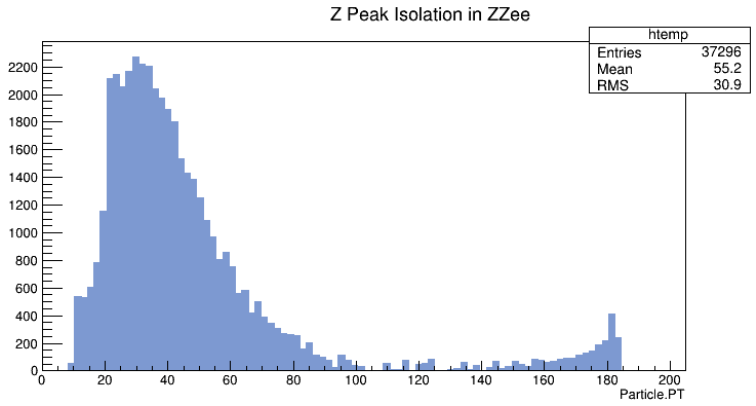

Figure 3: The ZZ pair is visible in the p_T distribution at 182GeV

Fig. 3. shows the peak in the p_T distribution of the leptons at 182 GeV against events, due to the ZZ production.

Fig. 4 is from a fully hadronic decay of W bosons and shows the sharp $t\bar{t}$ peak generated in $e + e- \rightarrow jets$. It is a standard background to generate and implement. At a mass of roughly 173 GeV, a $t\bar{t}$ pair would be near 350 GeV as is seen here.

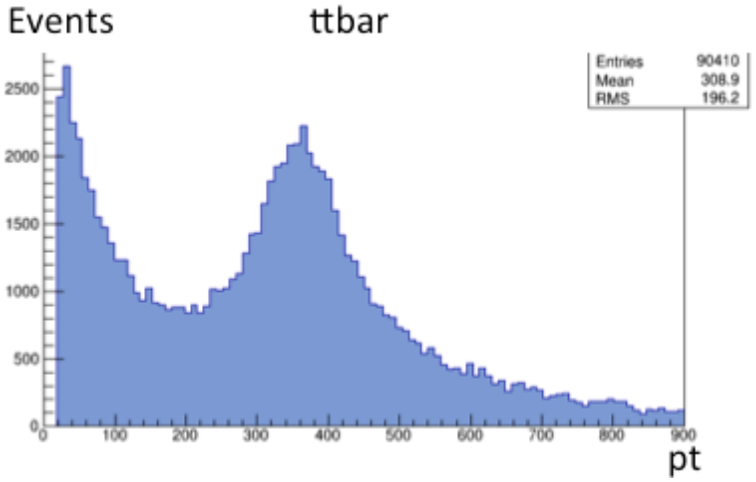

Figure 4: $t\bar{t}$ production at 350 GeV

Next, in Fig. 5 we can see the isolated peak of a WZ event against center-of-mass energy. Cuts were applied before generating this event which have reduced the signal on the order

of 65%. The signal is small, but necessary to remove as it is close to the WW pair signal.

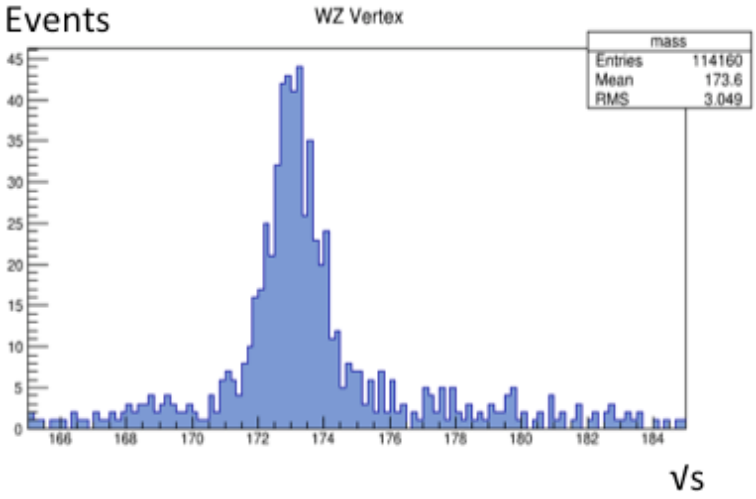

Figure 5: WZ peak isolation. Already, the event rate is rather low, though it will still obstruct the WW signal and must be cut.

Lastly in Fig. 7 the MET for 0-jet, 2-jet, and 4-jet events is shown without applied p_T cuts. One can see that an MET cut at and above 20 GeV all but removes the fully hadonically produced MET and reduced the $l\nu qq$ MET by nearly 20%. The fully leptonic channel is not easy to reconstruct however due to the two neutrinos present. Even worse still, if one of the leptons created is a tau, then a third neutrino will be produced making it nearly impossible to reconstruct. Therefore, we must employ the $q\bar{q}q\bar{q}$ or $q\bar{q}l\nu$ to accurately determine the leptonic momenta.

8 Probing the TGC Vertex

Now lets look at the TGC vertex. Similar to studies done at DØ which set Λ to 2TeV, it will be assumed that the ZWW and γWW couplings are equal in the case of the terms: g_V^1, $\Delta\kappa_V$, and λ_V where $V = Z, \gamma$. The transverse momentums are sensitive to the TGC vertices and so will be primarily addressed.

In Fig. 7 on the far left, the leading electron p_T is shown in two rather distinct instances. The distribution associated with the SM in blue and is synonymous with all parameters from the WWZ Lagrangian set identically to zero except for κ_V which is set to 1. The distribution formed from the dimension-6 operators has been set with all of the maximum values (furthest away from median predicted value since upper and lower error bars are different) given in the 2012 PDG. For instance, $\kappa_V = 0.928$, $\tilde{\lambda}_Z = -0.16$ etc. The center

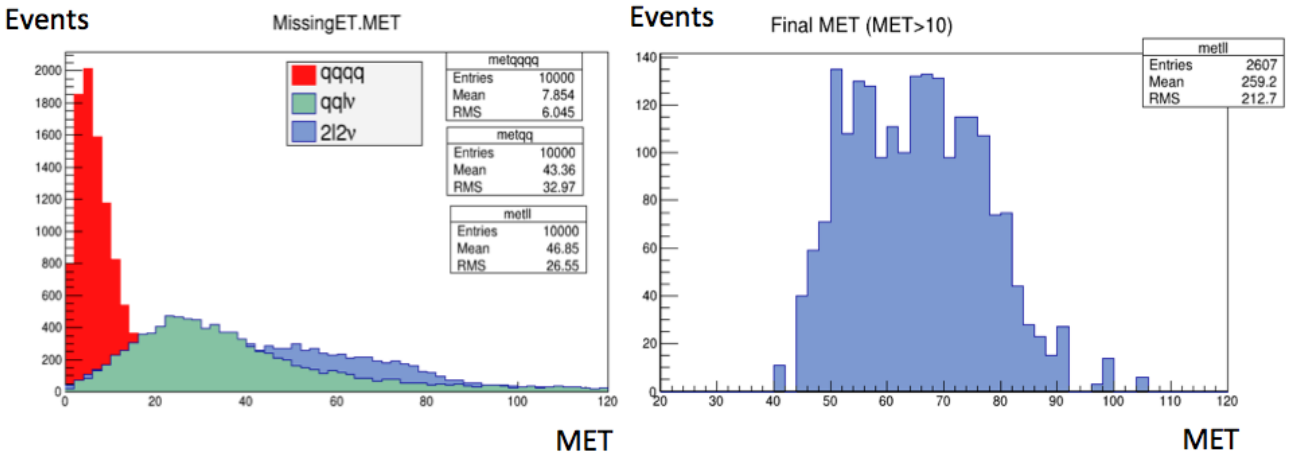

Figure 6: MET distributions showing an attempt to recover just the MET from the leptonic channel

distribution maintains the same parameters, but varies in λ_V slightly. The effects are not large, but since we know that these coupling should depend on the the CM energy, it suggests checking at higher energies for more significant deviations. Before seeing that however, note the far right plot. In this instance, the Dim. 6 prediction falls under the SM prediction. This negative correlation in general causes the cross section to decrease as well. Therefore it is a slightly more delicate matter to determine the multi-parameter fit as we may very well fit the SM with the wrong values.

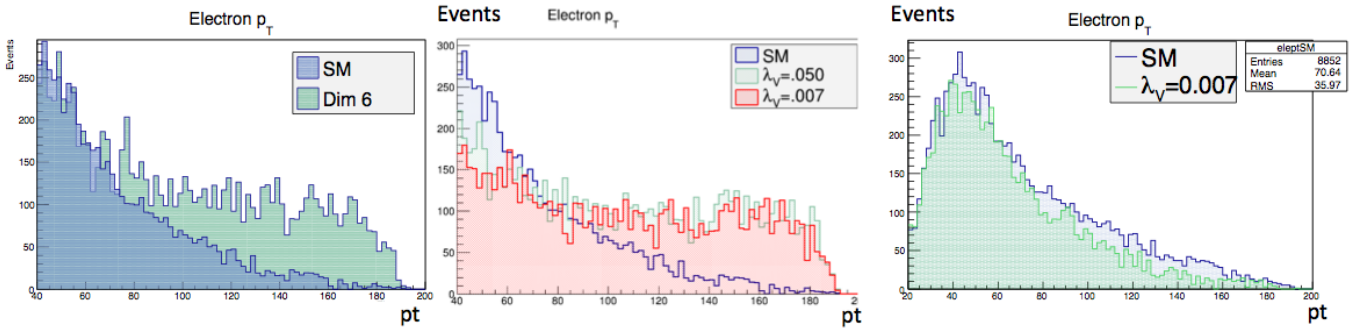

Figure 7: Plots showing various leading electron p_T distributions created by varying the TGC parameters as shown.

Knowing this, lets's take same parameters as in the two left distribution in Fig. 7 and

apply them at 1000 GeV center-of-mass energy and look at the distribution against the cross section. This is shown in Fig. 8. When the energies start getting comparable to the scale factor Λ we begin see a much larger deviation. The cross sections are quite similar up to around 150-200 GeV range, but the λ_V couplings, being dim-6, have a a strong dependence on the CM energy which is immediately evident.

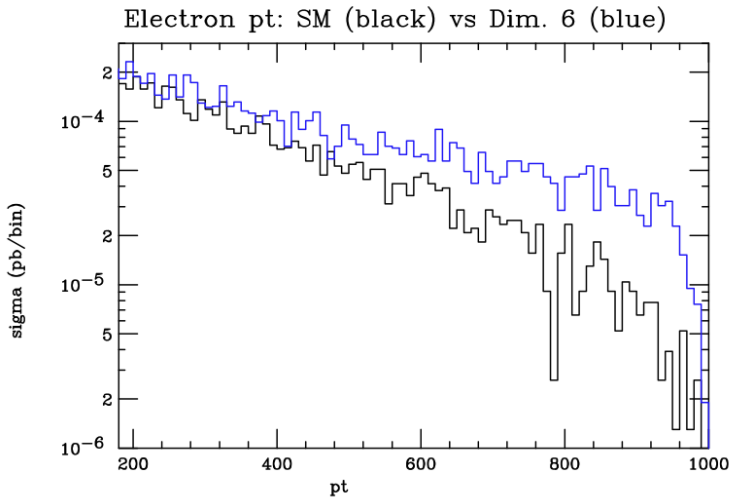

Figure 8: Relationship of the leading electron p_T against the cross section for the SM and Dim. 6 predictions

The distribution shown in Fig. 9 is (finally!) the isolated WW pair event for the CM energy (x-axis) against events (y-axis). As mentioned before, although the amount of events and branching ratios are low for the fully leptonic channel, the signal to background ratio is good. This here, consequently, was constructed out of these leptonic events, which allowed the WW pair to be reconstructed without having to lose too many events which could have otherwise passed the necessary criteria. Further, the Dim. 6 model was used with $\kappa_V = 0.983$ and $\lambda_Z = 0.007$.

Lastly, Fig. 10 plots the differences in the only to CP-violating parameters in the model. At CM energies near 200 GeV we are in a somewhat 'in-between' place where at higher energies, we must include diagrams with a Higgs in order to ensure the proper behavior of the cross section. And at lower energies, the polarization effects for a $(+,-)$ state are enhanced by a factor of $\sin\theta(1+\cos\theta)/(1-\cos\theta)$ and the, say, $e+$ will be preferentially emitted along the direction of the $W+$. So the $(+,-)$ combination will be peaked in the forward direction. These effects however cancel strongly as the energy is increased. So in order to better test the CP-violation (but not necessarily the TGC vertex) the energy should be increased. Though this matter won't be pursued further here.

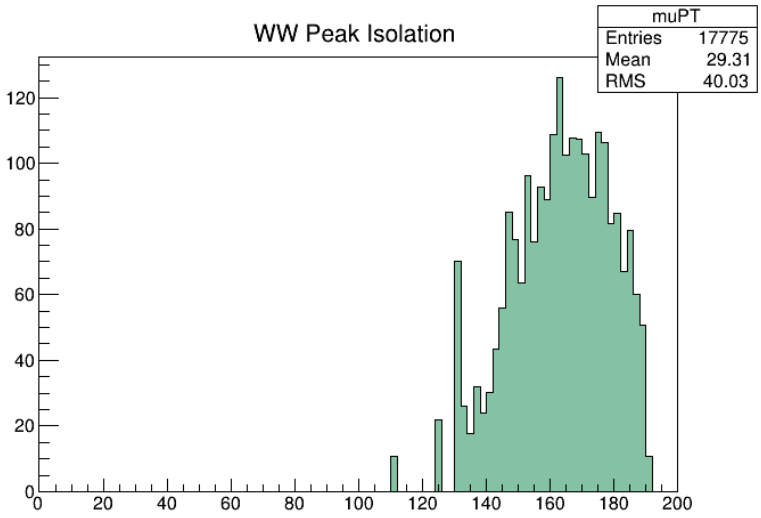

Figure 9: Signal at 162 GeV due to WW pair production from an $e+e-$ in-state. Number of events is on the y-axis and $\sqrt{s}$ on the x.

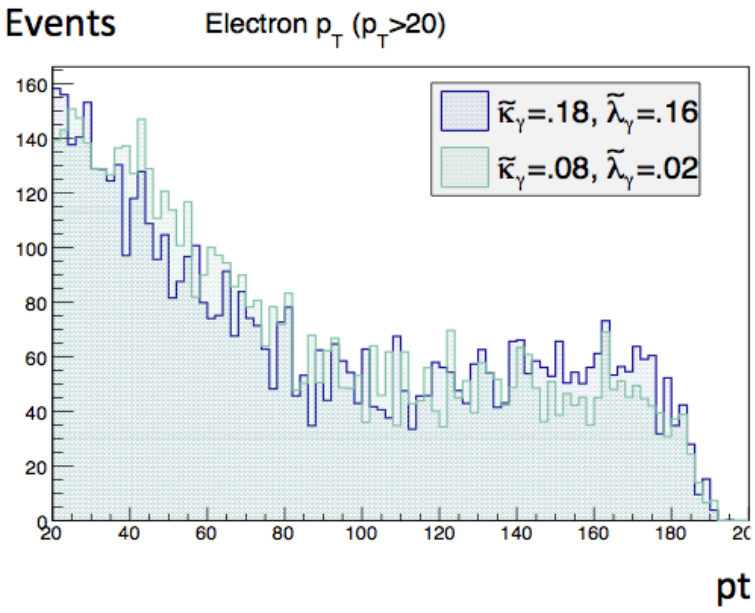

Figure 10: Various CP-violating distributions at 200 GeV CM energy. There is little variation at these energies, so an assumption that the parameters are 0 will indeed suffice in our model.

9 Predicting the W Mass

The use of new parameters causes a small shift in the mean predicted value of the W mass, however, we must remember that the coupling values used are as shown in Fig. 11 where the yellow band represents the 68% confidence limit their strength is dependent on the CM energy. Naturally then, shifting the value of λ_V can shift the mass very slightly. The current mean average of the mass given in the 2012 PDG is $M_W = 80.385 \pm 0.015$ GeV. The precision is really only 10^{-2}. Loop corrections within the SM on the vertex are at about the 10^{-3} level of precision. Therefore, at a low energy tree level calculation, the 400 MeV discrepancy of mean values is not especially statistically significant, though it highlights a possible route to look down to test BSM physics. We can perhaps get a somewhat better insight to what is happening here by looking a plot of the invariant WW mass as a function of the cross section at CERN. Using the Dim.6 model, they derived Fig. 12. There is indeed a variation in the invariant mass, though it is not as promising a route the search as what is presented next.

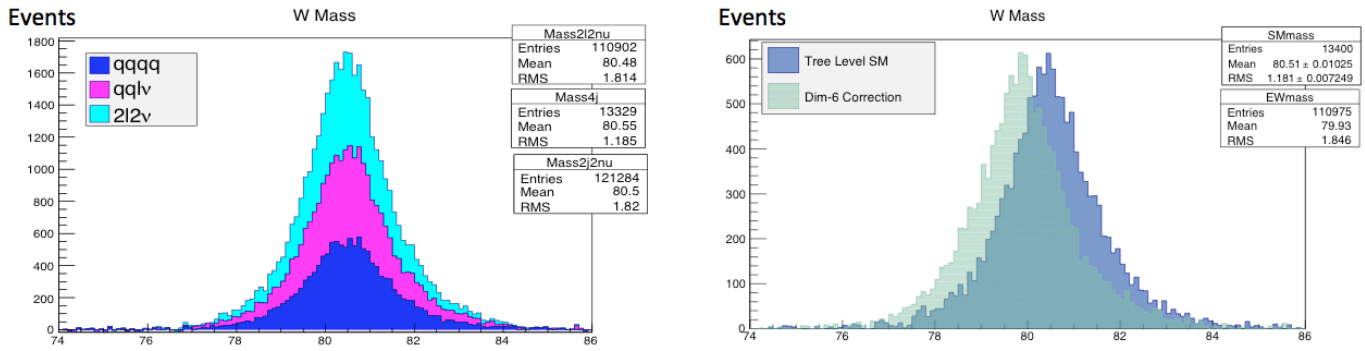

Figure 11: W mass distributions from various channels and the relationship between the Dim. 6 model and SM.

Finally, a look at ΔR in Fig. 13 which was acquired by a run at 1000 GeV with $\kappa_V = 0.983$ and $\lambda_Z = 0.050$ and the other parameters the same as in the tree-level SM. This represents of course the separation between decay products. The anomalous couplings show their effects in the lower regions which means that the decay products will be more collinear as the anomalous coupling is increased. In essence, if the W has a large transverse momentum, the decay products will tend to follow that direction. The cross section in the Dim. 6 model is larger than expected relative to the SM predictions. Therefore, to detect new physics, one should be moved to look at the co-linearity of the decay products at higher energies. The cross section is 'over-predictive' in the Dim. 6 model, therefore cross sections larger than expected from typical SM predictions may hint towards the true values of the anomalous coupling parameters and to BSM physics.

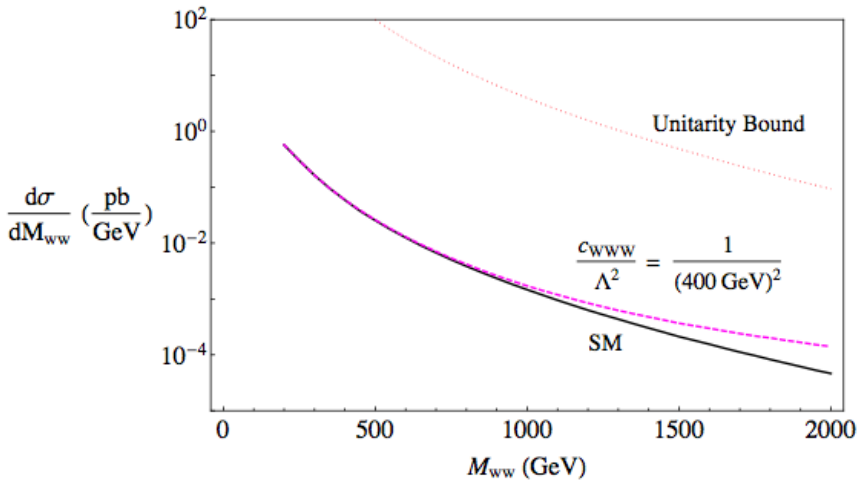

Figure 12: Splitting of the invariant WW mass as a function of Dim. 6 operators from CERN

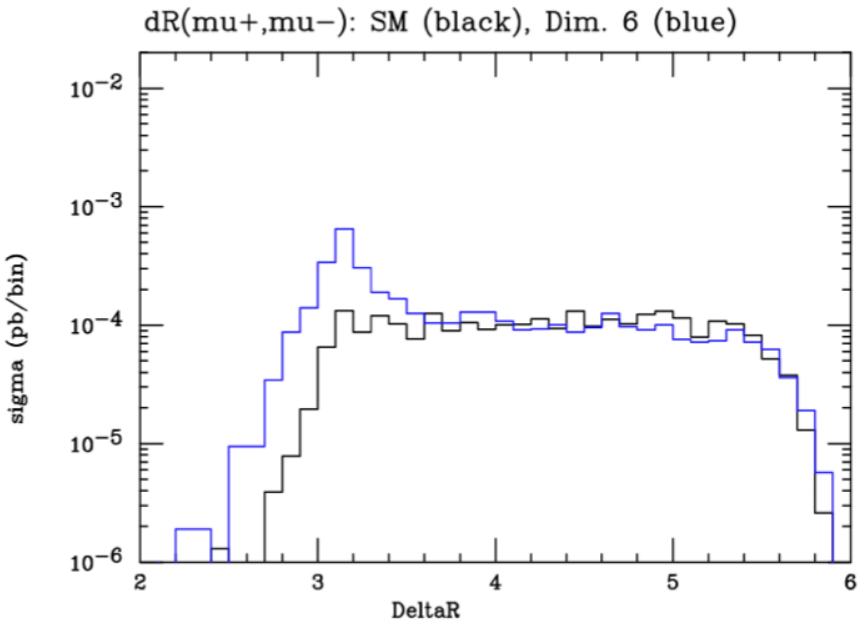

Figure 13: ΔR as a function of cross section showing itself as a promising place to look for BSM physics at high energies

10 Results

At lower energies, the effects the anomalous triple gauge coupling parameters is less evident, consistent with the predictions from the theory.

WW pair production via Z decay exists. This highly nonlinear problem resembles QCD in many respects and perhaps more similarities will revel themselves as we further our search into these vertices.

Backgrounds can be removed from the process by appropriate cuts and requirements without rejecting much of the desired signal.

Although these parameters are best tested at higher energies, they are able to more directly affect the vertex interactions and reveal extra information since they involve a multi-parameter fitting.

Some places to look for BSM physics are better than others. We expect the W's to come out back to back, same goes for the leptons and so probing ΔR is a great place to aim a search. Further, due to the intricate momentum dependencies of the TGC vertex, the transverse momentum distributions of the leptons provide detailed insight and noticeable deviations from SM predictions, suggesting that continued study should be directed here.

The multi-parameter fitting is flexible and allows terms which are explicitly zero in the tree-level SM to be non-zero (such as the CP-violating contributions). Variation of a parameter can be accomplished by changing the value of Λ. As this term increases, the limits on the parameters become better which is because the Λ scale is what ultimately determines to what degree the spreads and distributions are pushed towards the SM values.

It works! Perhaps not too surprising, however, it shows that there is plenty of room for discovery of new parameters. The probing of TGC vertices is still relatively young, and much more is yet to be learned.

11 Summary

The fusion into an electroweak theory leads directly to 3-point interactions which are foreign to pure QED and reveal a new realm of physics to be searched.

The TGC-couplings are open to accepting a model which includes numerous, very specific, parameters which can demonstrate specific aspects of these vertices.

Much is to be done! Future colliders running at high and higher energies will gradually hone in on the correct form of the WWZ Lagrangian and further reveal the true nature of the interaction.

An observable of the form

$$\delta = \frac{\sigma^{WW} - \sigma^{SM}}{\sqrt{\sigma^{SM}}}\sqrt{\mathcal{L}} \tag{33}$$

where $\mathcal{L}$ is the integrated luminosity in pb^{-1} and σ^{WW} is the $e+\ e- \to W+\ W-$

cross section, is an observable of potential new physics given in standard error units. It will prove to be very interesting to find out where exactly that value resides.

Additional colliders running $e+e- \to W+ W-$, $\gamma\ \gamma \to W+ W-$, and $p\bar{p} \to W+ W-$ will have much more to tell before long.

Thank you sincerely for your time and effort.
Respectfully,

Rich Ormiston